

Contents lists available at ScienceDirect

Organic Geochemistry

journal homepage: www.elsevier.com/locate/orggeochem



Spatiotemporal variations of organic matter sources in two mangrove-fringed estuaries in Hainan, China



Mengfan Chu a,b, Julian P. Sachs a,c, Hailong Zhang a,b, Yang Ding a,b, Gui'e Jin a,b, Meixun Zhao a,b,*

- ^a Frontiers Science Center for Deep Ocean Multispheres and Earth System, and Key Laboratory of Marine Chemistry Theory and Technology, Ministry of Education, Ocean University of China, Qingdao 266100, China
- b Laboratory for Marine Ecology and Environmental Science, Qingdao National Laboratory for Marine Science and Technology, Qingdao 266237, China
- ^c School of Oceanography, University of Washington, Box 355351, Seattle WA98195, USA

ARTICLE INFO

Article history:
Received 19 December 2019
Received in revised form 6 May 2020
Accepted 10 June 2020
Available online 24 June 2020

Keywords:
Blue carbon
Mangroves
Taraxerol
Lipid biomarkers
Stable carbon isotopes
Coastal biogeochemistry

ABSTRACT

Mangrove systems represent important long-term sinks for carbon since they have much higher carbon burial rates than terrestrial forests or typical coastal ecosystems. However, quantifying the sources of organic matter (OM) in estuarine and coastal sediments, where mangroves occur but are not the only source of OM, is challenging due to the variety of OM sources and diverse transport processes in these dynamic environments. The sources of OM in subtidal surface sediments of two mangrove-fringed estuaries in Hainan Province, China, were investigated using the mangrove-specific biomarker taraxerol and other lipid biomarkers, as well as stable carbon isotopes. Mixing models based on the concentration of taraxerol, plant wax n-alkanes and $\delta^{13}C_{OM}$ indicate that terrestrial non-mangrove plant OM accounted for 40-57% of the OM in the two estuaries, phytoplankton OM accounted for 24-45%, and OM from mangroves comprised 15-19% of the total. Terrestrial plants contributed 10-21% more of the OM to subtidal sediments of Bamen Bay, which is on the wetter, eastern side of Hainan Island, than to Danzhou Bay, but the phytoplankton OM fraction was 16-24% lower than that in Danzhou Bay subtidal sediments. In both estuaries, mangrove and phytoplankton OM fractions increased seaward while the terrestrial OM fraction decreased. On a seasonal basis, lipid biomarker concentrations indicated a small change of OM sources. The biomarker and carbon isotope approach used here can be applied to semi-quantitatively estimate spatial and temporal variations of the sources of organic carbon in tropical estuarine and coastal sediments, a major sink for carbon in the ocean.

© 2020 Elsevier Ltd. All rights reserved.

1. Introduction

Mangrove forests are ubiquitous along tropical coastlines and play an important role in coastal ecosystem health, but have been negatively impacted by anthropogenic activities (Li and Lee, 1996; McLeod et al., 2011). Mangrove forests also exchange vast quantities of organic matter (OM) between the land and sea and are of vital importance to regional and global carbon cycling (Jennerjahn and Ittekkot, 2002; McLeod et al., 2011). As one of the most carbon-rich forests on Earth, mangroves serve as a long-term carbon sink with much higher area-normalized carbon burial rates than terrestrial forests. The global mangrove carbon stock in 2012 was 4.19 ± 0.62 petagrams (Atwood et al., 2017; Hamilton and Friess, 2018). Broadly, the main sources of OM in

E-mail address: maxzhao@ouc.edu.cn (M. Zhao).

mangrove forests are terrestrial OM transported to the coastal zone by rivers, mangrove-produced OM such as leaves, roots, and wood, and aquatic OM that is produced in situ or imported by tides (Dale, 1974; Requejo et al., 1986; Meyers, 1997; Meziane and Tsuchiya, 2000; Alongi, 2014). Quantifying these sources of OM and their fate would help to better understand the carbon budgets in tropical and subtropical estuaries and coastal waters proximal to mangrove forests.

The origins and fates of OM in mangrove-fringed estuaries are often difficult to discern because of the multiple sources and their spatial heterogeneity, leading to a wide range of estimates. In most river deltas, terrestrial plants have been identified as the major OM contributors (Xu et al., 2006; Volkman et al., 2007; Carreira et al., 2016; Resmi et al., 2016). Mangrove-produced OM is either stored in situ above- or below-ground, or exported over short distances (Adame and Lovelock, 2011). Although mangroves have been recognized to contribute a significant proportion of OM to the local carbon budgets of tropical estuaries (Thimdee et al., 2003;

^{*} Corresponding author at: Key Laboratory of Marine Chemistry Theory and Technology (Ocean University of China), Ministry of Education, Qingdao 266100, China.

Gonneea et al., 2004), in most cases they are not the dominant OM source to sediments (Bouillon et al., 2004; Bouillon and Boschker, 2006). Substantial quantities of mangrove-derived OM are exported out of mangrove forests in some cases (Dittmar et al., 2001; Lugendo et al., 2007), while in other cases very little seems to be exported (Lee, 1995; Bouillon et al., 2008b). Apart from mangroves, other macrophytes including seagrass, macroalgae and saltmarsh plants contribute to OM storage in mangrove forests. Another complicating factor in apporitoning OM sources in tropical coastal systems is the tidal import of seagrass OM (Gonneea et al., 2004; Kennedy et al., 2004; Xu et al., 2006) that can reach 40% of total OM storage in mangrove forests (Prasad and Ramanathan, 2009). Aquatic algae can be the major source of particulate OM (Volkman et al., 2008; Tue et al., 2012; Bao et al., 2013a), but contribute minor amounts to sedimentary OM of mangrove systems (Alongi, 1994a, 1994b; Volkman et al., 2007; Meng et al., 2017).

Traditional proxies based on total organic carbon (TOC) and its stable isotopes have been applied to distinguish OM sources in mangrove systems (Thimdee et al., 2003; Prasad et al., 2017). For instance, Xue et al. (2009) used δ^{13} C and C/N (defined as the molar ratio of carbon to nitrogen) to investigate OM sources in a mangrove wetland in southern China, and concluded that 6-37% of sedimentary OM was derived from mangroves. However, due to the lack of a mangrove-specific OM indicator, this estimate included a mix of both mangrove- and terrestrial non-mangrove plant material. Lipid biomarkers can be useful to identify OM sources due to their source specificity and relative resistance to degradation. Examples are short chain (SC) and long chain (LC) n-alkanes, nalkanols and *n*-fatty acids (*n*-FAs), which are indicative of different plant sources (Eglinton and Hamilton, 1967; Cranwell et al., 1987; Jaffé et al., 2001). While these lipids can be used to fingerprint different vegetation OM, they can't adequately distinguish between OM from mangroves and terrestrial plants.

Pollen has been applied to trace mangrove OM in coastal systems, but can only settle into sediment when water velocity is low. Otherwise the transport of pollen, especially Rhizophora pollen, depends largely on wind (Franca et al., 2012). Owing to its dependence on source strength and transport processes pollen can be difficult to interpret in terms of mangrove OM source strength. In comparison, taraxerol, a well-preserved, sourcespecific lipid produced in large quantities by the leaves of Rhizophora spp. mangroves, has a great potential for providing more quantitative estimates of mangrove OM contributions (Cordeiro et al., 1999; Setzer et al., 2000; Adame and Lovelock, 2011; Koch et al., 2012; He et al., 2014). For example, Versteegh et al. (2004) used the ratios of taraxerol to the n- C_{29} alkane and the n- C_{28} alkanol, together with Rhizophora pollen, to distinguish sedimentary OM contributions from mangroves and terrestrial plants. Although taraxerol is relatively stable with respect to microbial degradation when compared to other molecular tracers for mangroves (Kristensen et al., 2008) it is likely, at least partially, to be oxidized to taraxerone and/or taraxerol acetate, or dehydrate to taraxerene during early diagenesis (Killops and Frewin, 1994; Pisani et al., 2013; He et al., 2018; Kumar et al., 2019). The extent to which taraxerol degrades to these and other products seems to vary by location. At one extreme, in near-surface sediments from the Potengi estuary in northeast Brazil, Kumar et al. (2019) observed taraxerol acetate to be the most abundant pentacyclic triterpenoid with no observable taraxerol present. In other locations, such as the Cross River estuary in southeast Nigeria and the Shark River estuary in Florida, USA taraxerol was far more abundant than taraxerone or taraxerol acetate (Pisani et al., 2013; He et al., 2018).

To date numerous studies have identified the variety of OM sources in mangrove systems, and documented their spatial distribution, but few have quantified the different OM proportions. Here, lipid biomarkers, δ^{13} C values of TOC, and several molecular proxies

including CPI_{alk}, Paq, ACL_{alk} and BIT were used to identify the sources of OM in two mangrove-fringed estuaries in Hainan Province, China that differ in their annual precipitation by 29%. Then mixing models were employed to provide more quantitative estimates of these sources. Taraxerol was used as a biomarker specifically to quantify the contribution of the common *Rhizophora* spp. mangroves to local sedimentary OM. The objectives of this investigation were to: (1) identify and quantify the input of OM from different sources; (2) explore a new application of taraxerol to apportion OM sources in mangrove-fringed estuaries; and (3) compare the temporal and spatial variations of OM input within and between two nearby estuaries receiving different amounts of rainfall.

2. Materials and methods

2.1. Study areas

Bamen Bay (BMB) is located in Qinglan Harbor, Wenchang City, Hainan Province of China (Fig. 1). Located on the east coast of Hainan Island, BMB experiences the most frequent and severe typhoon-induced storm surge disasters in the South China Sea region (Wang et al., 2018). The mangrove forest area in BMB is 1223 km² in the National mangrove nature reserve established in 1981 (Chen et al., 2017). It is also an important aquaculture area in Hainan province (Bao et al., 2013b). BMB contains one of the largest mangrove forests on Hainan Island (Zhang and Sui, 2001), where *Rhizophora apiculata* represents one of the most common mangroves in the study area (Chen and Chen, 1998; Liao et al., 2000; Nong et al., 2011).

Danzhou Bay (DZB) is a semi-closed inner bay of the Beibu Bay, located in Danzhou City, Hainan Province of China. DZB is a municipal natural reserve of mangroves, possessing 133 km² of mangrove coverage and a high abundance of *Rhizophora stylosa*, the dominant mangrove species (Wu et al., 2016; Chen et al., 2017).

Both estuaries have a wet summer and dry winter climate, with precipitation during the wet season (May–Oct.) accounting for roughly 80% of annual precipitation. The large (29%) precipitation difference between BMB (1838 mm/yr) and DZB (1426 mm/yr) provides a starting point for ascertaining how rainfall rates may influence OM source strengths and apportionment. Meanwhile the wide geographic distribution of *Rhizophora* spp. make these estuaries suitable for applying a taraxerol-based proxy for mangrove OM input to sediments. Additional information on the physical characteristics and mangrove distributions in BMB and DZB, as well as the most common vascular plants on Hainan Island can be found in Supplementary Tables S1 and S2.

2.2. Sampling

Surface sediments were collected in subtidal areas in boreal summer (July 20–25) and autumn (November 9–11) of 2016. Sample stations were named in downstream sequence from freshwater to seawater. Seaward distance here refers to the distance from the sampling site to the mouth of the bay (indicated by dashed lines in Fig. 1). Salinity was measured with a hand-held conductivity meter (WTW Multi 3420. Supplementary Fig. S1).

Significant sediment differences were visible between BMB and DZB. DZB samples were sandy clay or coarse sands mixed with shells and plant debris. In BMB, four of 13 sediment samples contained sand and shells (BMB summer-1, 4, 5, 6), with the remainder being dark clay mixed with plant debris.

Fresh mature *Rhizophora* mangrove leaf samples (*R. apiculata* in BMB and *R. stylosa* in DZB) were collected in each estuary during

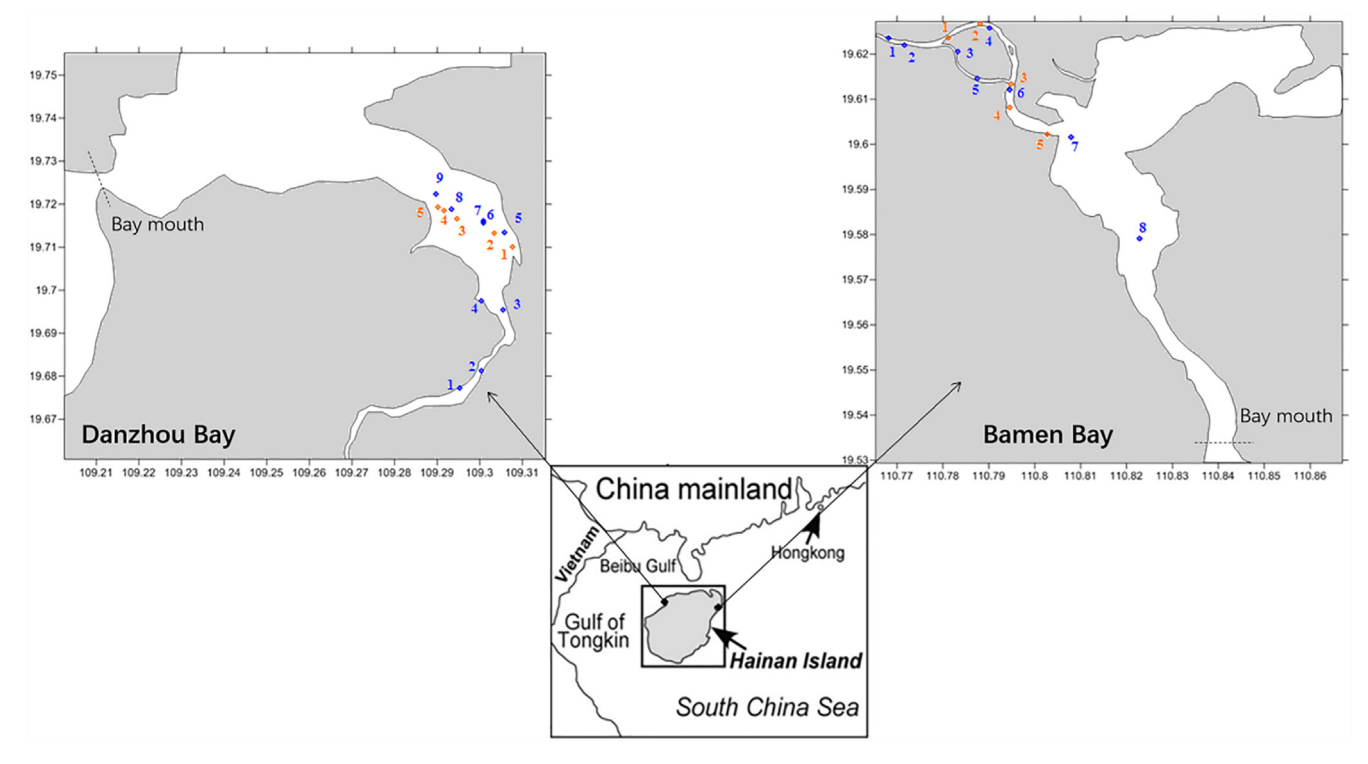


Fig. 1. Map of BMB and DZB. Background figure from Mao et al. (2006). Blue: summer sampling stations; orange: autumn sampling stations. Distance to sea from each site was measured from the location marked as "bay mouth". (For interpretation of the references to colour in this figure legend, the reader is referred to the web version of this article.)

the autumn 2016 field campaign. All samples were stored at $-20\,^{\circ}\text{C}$ before treatment.

2.3. Analytical methods

2.3.1. TOC analysis

All samples were freeze-dried and ground to a fine powder before total organic carbon (TOC) and lipid biomarker analysis. For TOC, samples were acidified with 4 M HCl at room temperature to remove inorganic carbon and then rinsed with purified (Milli-Q) water repeatedly until a pH of 7 was reached, then dried at 55 °C and re-ground. TOC was measured on a Thermo Flash 2000 Elemental Analyzer.

The standard deviations for repeated analyses of laboratory standards (Atropina Standard (TOC = 70.56%) and Low Organic Content Soil Standard OAS (TOC = 1.55%)) were \pm 0.02 wt% (n = 6) for TOC and \pm 0.002 wt% (n = 6) for total nitrogen (TN).

2.3.2. Lipid biomarker analysis

Approximately 1 g (dry mass) of sediments or 0.1 g of leaf tissue were extracted 6 times with dichloromethane (DCM) and methanol (MeOH) (3:1, v/v) by ultrasonication after adding n-C₁₉ alkanol, deuterium-substituted n-C₂₄ alkane, n-C₁₉ fatty acid (FA), and C₄₆ glycerol dialkyl glycerol tetraether (GDGT) as internal standards. The supernatants were collected by centrifugation, solvents were evaporated, then the total lipid extracts were hydrolyzed with 6% KOH in methanol.

Neutral lipids were extracted with hexane and fractionated into apolar (alkanes) and polar (alkanols, alkenones, sterols and GDGTs) fractions using solid phase extraction on silica gel and eluting first with hexane, followed by DCM/methanol (95:5, v/v). The apolar fraction was taken to dryness under a stream of N_2 , then redissolved in isooctane before analysis of alkanes by gas chromatography with flame ionization detection (GC-FID). The polar fraction

was divided into 3 parts. The first was condensed and derivatized with N,O-bis(trimethylsily)-trifluoroacetamide (BSTFA) before GC-FID analysis of alkanols (as silyl ethers), sterols (as silyl ethers), and alkenones. The second fraction was derivatized with acetic anhydride and pyridine for measurement of taraxerol (as an acetate) via GC-FID. The third was re-dissolved in 500 μL isopropanol/hexane (5:95, v/v) prior to filtration with a PTFE 0.45 μm filter and injection on a high performance liquid chromatograph–mass spectrometer (HPLC–MS) for GDGT measurements.

FAs were extracted into hexane after adding 6 M HCl to the aqueous phase. After repeated sonication, centrifugation and solvent evaporation, FAs were transesterified with HCl in methanol (5:95, v/v), then extracted into hexane. FAs were concentrated and dissolved in isooctane before GC analysis.

2.3.3. GC, EA-IRMS and HPLC-MS analysis

n-Alkanes, n-alkanols, taraxerol and n-FAs were quantified on an Agilent 6890 N GC with an FID and a silica capillary column (HP-1 methyl siloxane, 50 m, 0.32 mm i.d. and 0.17 μ m film thickness). Hydrogen was used as carrier gas with a flow rate of 1.0 mL/min. The oven temperature was programmed such that 80 °C was held for 1 min, then heated at 25 °C/min to 200 °C, followed by heating at 4 °C/min to 250 °C, 1.7 °C/min to 300 °C where it was held for 10 min, and 5 °C/min to 315 °C where it was held for 5 min

The stable carbon isotopic composition ($^{13}C/^{12}C$) of TOC was measured using an elemental analyzer-isotope ratio mass spectrometer (EA-IRMS) system. $^{13}C/^{12}C$ ratios were reported in the delta notation ($\delta^{13}C$) calibrated to the Peedee belemnite (PDB) standard with a standard deviation of 0.06% (n = 6) based on repeated measurements of laboratory standards (USGS 40 ($\delta^{13}C = -26.39\%$), IAEA 600 ($\delta^{13}C = -27.77\%$) and IAEA-CH₃ ($\delta^{13}C = -24.72\%$)) and a laboratory working standard

 $(\delta^{13}C = -23.76\%)$, which were run after every 10 authentic samples. Precision was better than $\pm 0.2\%$ for the IRMS system based on repeated analyses of the standards.

GDGTs were quantified with an Agilent 1200 series HPLC equipped with a triple quadrupole mass spectrometer (Waters-Quattro Ultima Pt) operated in atmospheric pressure chemical ionization (APCI) mode. Separation of individual GDGTs was achieved on a Prevail cyano column (150 mm \times 2.1 mm, 3 µm, Grace) at 30 °C. GDGTs were eluted isocratically with hexane and hexane/ isopropanol (9:1, v/v) at a flow rate of 0.3 mL/min. Operating conditions for the APCI-MS were as follows: corona 6 µA, source temperature 95 °C, cone voltage 35 V, APCI probe temperature 550 °C, cone gas (N2) flow 90 L/h, desolvation gas (N2) flow 600 L/h. Selected Ion Recording (SIR) was used to detect the protonated molecules $[M+H]^+$ (dwell time = 50 ms) of GDGTs (m/z 1302; 1300; 1298; 1296; 1292; 1050; 1036; 1022; 744 (C46 GDGT, internal standard)).

2.4. Biomarkers and proxies

All biomarkers and the proxies based upon them are listed in Table 1.

2.5. Statistical treatments

IBM SPSS Statistic software was used to compute linear regression results and Student's t test of significance. The MATLAB package by Bosch et al (2015) was adapted to apportion the OM sources in the three-endmember mixing model using a Bayesian Markov chain Monte Carlo method.

3. Results

3.1. TOC content, C/N and δ^{13} C

In BMB, TOC values of the surface sediments varied between 0.5% and 2.9% (avg. \pm std = 2.0 \pm 1.1%, n = 5 and hereafter; Table 1) in the autumn, and between 0.3% and 7.0% (avg. \pm std = 2.8 \pm 2.5%, n = 8 and hereafter) in the summer (Table 2). Weight-based C/N values were between 10.6 and 15.5 (avg. \pm std = 12.1 \pm 2.0) in the

autumn, and between 9.5 and 18.8 (avg. \pm std = 13.6 \pm 3.7) in the summer. The range of $\delta^{13}C$ values was -27.6% to -26.1% (avg. \pm std = $-26.6 \pm 0.6\%$) in the autumn and -28.2% to -23.6% (avg. \pm std = $-26.0 \pm 1.6\%$) in the summer.

In DZB, TOC values ranged from 0% to 2.0% (avg. \pm std = 0.8 \pm 0.8%, n = 5 and hereafter) in the autumn and 0% to 0.5% (avg. \pm std = 0.4 \pm 0.4%, n = 9 and hereafter) in summer. Most DZB samples had TN values below the detection limit, or < 0.01%. The range of δ^{13} C values was -26.7% to -23.6% (avg. \pm std = $-24.9 \pm 1.3\%$) in the autumn and -25.9% to -21.9% (avg. \pm std = $-24.2 \pm 1.5\%$) in the summer.

TOC content was negatively correlated with $\delta^{13}C$ values in both estuaries (Supplementary Fig. S2).

3.2. Lipid biomarker concentrations

Lipid biomarker concentrations were normalized to TOC to minimize the impact of different mineral and non-organic fluxes across the sampling regimes and are listed in Supplementary Tables S3-S5. In BMB, *n*-alkanes exhibited an odd/even predominance, with an average concentration of $329 \pm 62 \mu g/g$ TOC (n = 5) in the autumn and 305 ± 104 μ g/g TOC (n = 8) in the summer. n-C₂₉, n- C_{31} and n- C_{33} were the most abundant alkanes in both seasons (Fig. 2A, Supplementary Table S3). n-alkanols exhibited an even/ odd predominance (Fig. 2A, Supplementary Table S4). The average *n*-alkanol concentration was $1267 \pm 566 \mu g/g$ TOC in the autumn, and $1359 \pm 734 \,\mu\text{g/g}$ TOC in the summer, with the $n\text{-}\text{C}_{28}$ alkanol the most abundant n-alkanol in both seasons. The concentration of short-chain n-fatty acids (C_{13} - C_{18} ; SCFA) averaged $432 \pm 137 \,\mu\text{g/g}$ TOC in the autumn and $1412 \pm 776 \,\mu\text{g/g}$ TOC in the summer. The concentration of long-chain fatty acids $(C_{20}-C_{33}; LCFA)$ averaged 528 ± 179 µg/g TOC in the autumn and $1237 \pm 573 \,\mu\text{g/g}$ TOC in the summer (Fig. 2A, Supplementary Table S5). LCFAs showed an odd/even predominance. The most abundant LCFA was $n-C_{28}$ FA in the autumn and $n-C_{24}$ FA in the summer. n-FAs were more abundant in summer than in autumn, with the concentration of major components (n- C_{16} C_{24} and C_{26} FAs) nearly twice that in autumn samples.

In DZB, n-alkane concentrations averaged 871 \pm 1080 μ g/g TOC (n = 5) in the autumn and 524 \pm 357 μ g/g TOC (n = 9) in the

Table 1Biomarkers and proxies used in this paper. References for lipid proxies can be found in Volkman and Smittenberg (2017).

Biomarkers or proxies		Main sources				
n-alkyl lipids	Long-chain alkanes ($C_{23} - C_{37}$) Long-chain alkanols ($C_{22} - C_{30}$) Long-chain fatty acids ($C_{20} - C_{33}$)	Vascular plants				
	Short-chain alkanes $(C_{18} - C_{22})$	Aquatic phytoplankton				
Triterpenoids	Taraxerol	Rhizophora mangrove				
Sterols	Brassicasterol/epi-brassicasterol	Diatom & phytoplankton				
	Dinosterol	Dinoflagellates				
Alkenones	C _{37:2,37:3} alkenones	Haptophyte algae				
Glycerol dialkyl glycerol tetraethers (GDGTs)	branched glycerol dialkyl glycerol tetraether (br-GDGTs)	Soil and riverine OM				
	Crenarchaeol	Marine pelagic Crenarchaeaota				
LC-alkanols = n -C ₂₆ alkanol + n -	-C ₂₈ alkanol + n-C ₃₀ alkanol	Vascular plants				
PB = brassicasterol or epi-brass	icasterol + dinosterol + C _{37:2,37:3} alkenones	Marine phytoplankton				
$T = taraxerol/n-C_{31}$ alkane		Relative contribution of Rhizophora mangrove OM to total vascular plant OM				
$Paq = \Sigma (n-C_{23} + n-C_{25} \text{ alkanes})$	$\Sigma (n-C_{23} + n-C_{25} + n-C_{29} + n-C_{31} \text{ alkanes})$	Relative OM contribution of non-emergent aquatic macrophyte to emergent aquatic and terrestrial plants				
$CPI_{26-33} = \sum (n-C_{27} + n-C_{29} + n-C$	$C_{31} + n$ - C_{33} alkanes)/ Σ (n - $C_{26} + n$ - $C_{28} + n$ - $C_{30} + n$ - C_{32}	Relative OM contribution of vascular plant				
ACL _{alk} = Σ (i*X _i)/ Σ X _i (where X from 18 to 37)	is abundance and i represents the carbon number					
III)/(br-GDGT-I + br-GDGT-II	etraether) = (br-GDGT-I + br-GDGT-II + br-GDGT-II + br-GDGT-III + crenarchaeol) (Structures of DGTs in Supplementary Fig. S3)	Relative OM contribution of mainly soil and riverine production to marine phytoplankton production				

 Table 2

 Bulk characteristics of surface sediments and leaf samples.

Station No.	Salinity (ppt)	Rhizophora measured	Surface sediments			Leaf samples				
			δ ¹³ C (‰)	TOC (%)	TN (%)	C/N	δ ¹³ C (‰)	TOC (%)	TN (%)	C/N
BMB autumn-1	0.3	Rhizophora apiculata	-26.9	2.9	0.3	11.1	-31.6	45.7	1.6	28.1
BMB autumn-2	1.5	Rhizophora apiculata	-27.6	2.3	0.2	12.3	-31.9	43.7	2.3	19.1
BMB autumn-3	2.2	Rhizophora apiculata	-26.2	1.3	0.1	10.6	-29.3	44.5	1.4	32.7
BMB autumn-4	4.1	Rhizophora apiculata	-26.1	2.9	0.3	11.1	-28.9	45.8	1.7	27.6
BMB autumn-5	17.6		-26.2	0.5	0.0	15.5				
BMB autumn avg. ± std			-26.6 ± 0.6	2.0 ± 1.1	0.2 ± 0.1	12.1 ± 2.0	-30.4 ± 1.3	45.0 ± 0.9	1.7 ± 0.3	26.9 ± 4.9
DZB autumn-1	7.3	Rhizophora stylosa	-24.4	0.9	0.1	13.6	-28.8	45.2	1.1	42.1
DZB autumn-2	10.1	Rhizophora stylosa	-25.6	1.0	0.1	13.4	-27.8	42.7	1.3	33.0
DZB autumn-3	8.6	Rhizophora stylosa	-26.7	2.0	0.1	13.7	-29.1	42.9	1.3	32.8
DZB autumn-4	11.1	Rhizophora stylosa	-24.0	0.0	0.0	N/A	-29.1	41.9	1.3	33.1
DZB autumn-5	14.7	Rhizophora stylosa	-23.6	0.0	0.0	N/A	-28.6	45.0	1.4	31.5
DZB autumn avg. ± std			-24.9 ± 1.3	0.8 ± 0.8	0.1 ± 0.1	13.6 ± 0.2	-28.7 ± 0.5	43.5 ± 1.5	1.3 ± 0.1	34.5 ± 4.3
BMB summer-1	7.0		-26.2	0.3	0.0	16.8				
BMB summer-2	7.5		-28.1	6.4	0.4	15.8	-29.7	49.8	1.4	35.8
BMB summer-3	15.6	Rhizophora apiculata	-28.2	7.0	0.4	16.1				
BMB summer-4	13.0	Rhizophora apiculata	-25.9	1.2	0.1	9.5	-28.1	51.9	1.6	33.2
BMB summer-5	24.0	Rhizophora apiculata	-25.7	2.0	0.2	9.5	-30.1	45.9	1.8	25.2
BMB summer-6	26.0	Rhizophora apiculata	-24.3	0.5	0.0	18.8	-30.0	50.0	1.4	34.9
BMB summer-7	27.5	Rhizophora apiculata	-26.2	2.8	0.2	12.0	-27.5	47.1	1.1	42.2
BMB summer-8	32.8	Rhizophora apiculata	-23.6	2.4	0.2	10.0				
BMB summer avg. ± std			-26.0 ± 1.6	2.8 ± 2.5	0.2 ± 0.2	13.6 ± 3.7	-29.1 ± 1.2	48.9 ± 2.4	1.5 ± 0.3	34.3 ± 6.1
DZB summer-1	0.1		-24.0	0.1	0.0	N/A				
DZB summer-2	0.2		-21.9	0.1	0.0	N/A				
DZB summer-3	0.9	Rhizophora stylosa	-22.7	0.3	0.0	N/A	-27.7	51.4	1.5	34.1
DZB summer-4	0.7	Rhizophora stylosa	-23.7	0.3	0.0	N/A	-28.2	50.4	1.7	29.8
DZB summer-5	7.8	Rhizophora stylosa	-25.5	0.4	0.0	N/A	-29.2	52.5	2.0	25.7
DZB summer-6	4.0	Rhizophora stylosa	-25.8	0.5	0.0	N/A	-29.9	53.1	1.6	32.2
DZB summer-7	7.2	Rhizophora stylosa	-25.9	1.4	0.0	N/A	-28.4	49.3	1.2	40.7
DZB summer-8	7.0		-25.5	0.1	0.0	N/A				
DZB summer-9	7.0		-22.6	0.0	0.0	N/A				
DZB summer avg. ± std			-24.2 ± 1.5	0.4 ± 0.4	0.0 ± 0.0		-28.7 ± 0.9	51.3 ± 1.5	1.6 ± 0.3	32.5 ± 5.6

summer, with n- C_{29} , C_{31} , and C_{33} as the most abundant alkanes in autumn and n-C₂₇, C₂₉, C₃₁ as the most abundant alkanes in summer (Fig. 2B, Supplementary Table S3). n-alkanol concentrations averaged $1591 \pm 1657 \,\mu\text{g/g}$ TOC in the autumn $1370 \pm 397 \,\mu\text{g/g}$ TOC in the summer, with $n\text{-}C_{28}$ alkanol as the most abundant in both seasons (Fig. 2B, Supplementary Table S4). The total *n*-FA concentration was much higher in DZB than in BMB. Average SCFA concentrations in DZB were $3366 \pm 3394 \,\mu g/g$ TOC in autumn and $3845 \pm 3338 \,\mu g/g$ TOC in summer, while those of LCFAs were $6513 \pm 9792 \,\mu\text{g/g}$ TOC in autumn and 1470 ± 980 μg/g TOC in summer (Fig. 2B, Supplementary Table S5). The most abundant LCFA was n- C_{26} in autumn and n-C₂₄ FA in summer. Several of the DZB samples (e.g., autumn-4, summer-2 and summer-4) had high concentrations of n-C₂₅ FA that were not observed in leaves. As in BMB, DZB samples displayed an odd/even predominance for n-alkanes and an even/odd predominance for n-alkanols. Apart from a high n-C₂₅ FA concentration in some samples, LCFAs exhibited an even/odd predominance in all samples.

LC-alkanols (n-C₂₆, C₂₈, C₃₀), taraxerol and the phytoplankton biomarkers brassicasterol/epi-brassicasterol + dinosterol + C_{37:2}, C_{37:3} alkenones (PB) were used to represent the input of OM from higher plants, mangroves, and aquatic microalgae, respectively (Fig. 3). In BMB sediments, TOC-normalized concentrations of LC-alkanols, taraxerol and PB averaged 982 ± 545 μ g/g TOC, 284 ± 289 μ g/g TOC, and 172 ± 42 μ g/g TOC (n = 5) in the autumn, compared to 1055 ± 624 μ g/g TOC, 159 ± 135 μ g/g TOC, and 107 ± 45 μ g/g TOC (n = 8) in the summer, respectively. Autumn samples had higher taraxerol and PB concentrations and lower LC-alkanol concentrations. For DZB samples, concentrations of LC-alkanols, taraxerol and PB averaged 1138 ± 1227, 1878 ± 1842, 139 ± 175 μ g/g TOC (n = 5) in the autumn and 831 ± 391 μ g/g TOC, 762 ± 957 μ g/g TOC, and 383 ± 263 μ g/g TOC (n = 9) in the

summer, respectively. Both LC-alkanols and taraxerol were more abundant in the autumn, but summer PB concentrations were twice that of autumn concentrations.

3.3. Biomarker-based indexes

3.3.1. ACLalk, CPIalk, Paq and BIT

The four biomarker-based indices ACL_{alk}, CPI_{alk}, Paq and BIT were used to apportion subtidal sedimentary OM in the two estuaries to different sources, as defined in Table 1 (Eglinton and Hamilton, 1967; Poynter and Eglinton, 1990; Ficken et al., 2000; Hopmans et al., 2004).

BMB samples had significantly higher ACL_{alk} and lower Paq values than DZB samples (p < 0.01, Fig. 4, Supplementary Table S6). The BMB CPl_{alk} values ranged from 2.9 to 5.7, ACL_{alk} values from 28.5 to 29.7, BIT values from 0.6 to 0.9, and Paq values from 0.1 to 0.3. The DZB samples had CPl_{alk} values ranging from 0.9 to 4.3, ACL_{alk} values from 25.6 to 29.1, BIT values from 0.6 to 1.0, and Paq values from 0.2 to 0.7. Autumn samples in BMB had lower ACL_{alk} values. Autumn samples in DZB generally had higher CPl_{alk} and lower Paq values than summer samples. BIT values in summer samples of both BMB and DZB showed a linear correlation with the distance to bay mouth (r = 0.85 and 0.93, respectively; Supplementary Table S6).

3.3.2. Taraxerol-based proxies

To provide an estimate of the relative proportion of higherplant OM derived from *Rhizophora* spp. mangroves, we calculated the ratio of taraxerol to the most abundant n-alkane (which was n- C_{31} in all but DZB summer samples-1, 2, and 7) in *Rhizophora* leaf samples collected during the autumn sampling period (defined as $T = \frac{\tan x \cot n - C_{31}}{\ln x}$ alkane since all vascular plants produce n- C_{31} alkane but *Rhizophora* trees are the primary

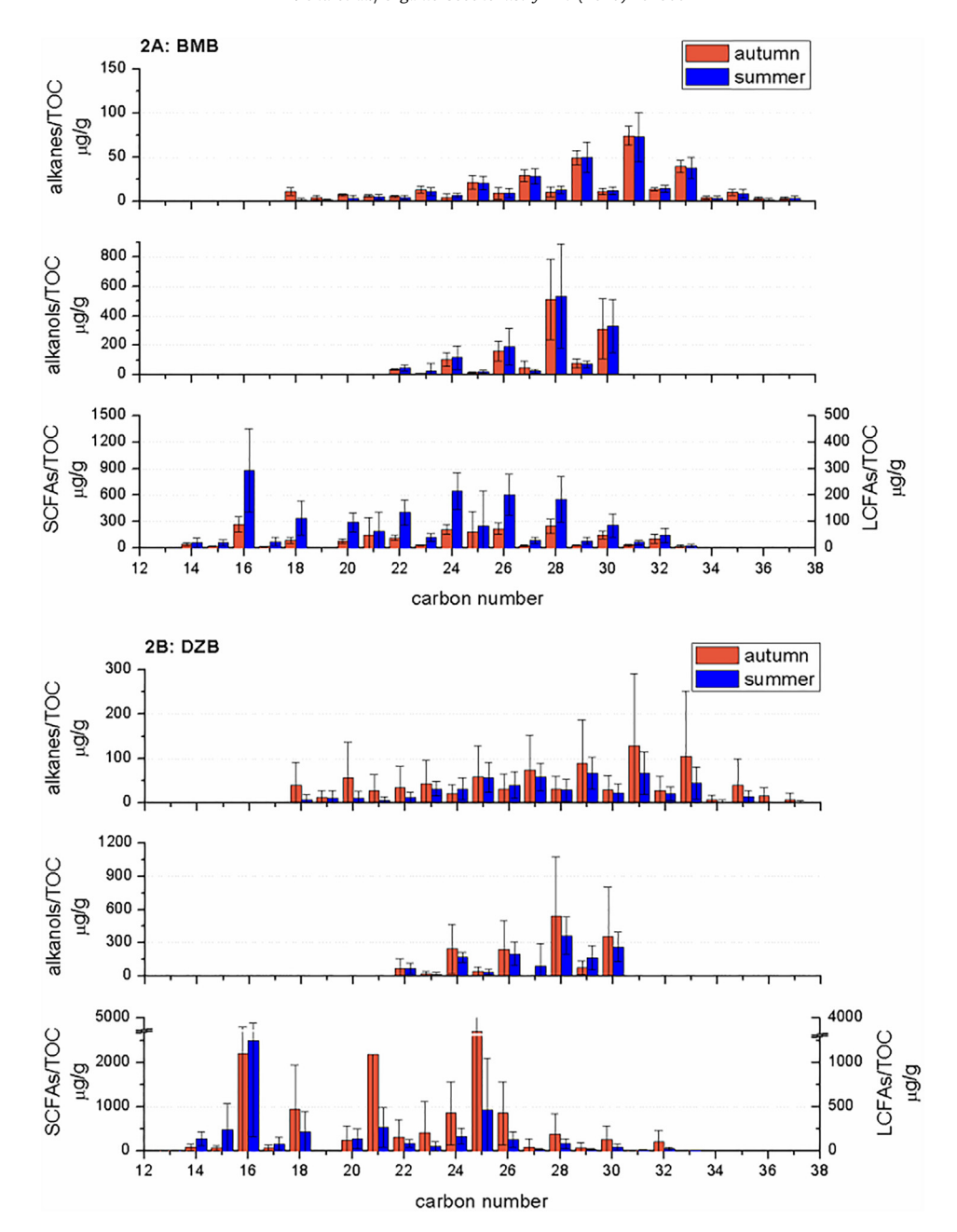


Fig. 2. TOC normalized concentration of lipid biomarkers. 2A and 2B for n-alkanes, n-alkanels and n-FAs in BMB and DZB, respectively. The error bars indicate the standard deviation of the average across all sites. Short-chain fatty acids (SCFA) are those with carbon numbers between n-C $_{13}$ and n-C $_{18}$, while long-chain fatty acids (LCFA) are those with carbon numbers between n-C $_{20}$ and n-C $_{33}$. Data for each site and season are listed in Supplementary Tables S3–S5.

producer of taraxerol) and compared those to the same ratio in sediments. Rhizophora leaves from BMB had lower T values $(avg. \pm std = 90 \pm 32,$ n = 4than those from DZB (avg. \pm std = 280 \pm 69, n = 4) despite the taraxerol concentrations leaves from both estuaries being similar (avg. \pm std = 7254 \pm 2111 and 9182 \pm 3414 μ g/g TOC for BMB and DZB, respectively; Table 3). Sedimentary T values in BMB averaged $4.0 \pm 3.7 \ (n = 5)$ in autumn and $3.0 \pm 1.4 \ (n = 8)$ in summer. T values in DZB were 5–10 times greater, averaging 22 ± 25 (n = 5) in autumn and 32 ± 27 (n = 9) in summer (Table 3).

The ratio of T values of subtidal sediment samples to those of *Rhizophora* leaf samples was calculated. In BMB, this ratio averaged $4.5\pm4.0\%$ (n = 5) in the autumn and $2.7\pm1.5\%$ (n = 8) in the summer. In DZB, the ratio averaged $7.9\pm9.0\%$ (n = 5) in the autumn and $5.3\pm8.7\%$ (n = 9) in the summer (Table 3).

3.4. OM source quantification

3.4.1. Endmember values

Apportioning the sources of OM to sediments with biomarker and isotopic values requires the definition of appropriate endmember values (Table 4). For the phytoplankton endmember, we applied an average $\delta^{13}C$ value of $-20.8\pm0.4\%$ from the phytoplankton in the northern SCS, which was used as the marine endmember to characterize sources of OC in the Pearl River Estuary by He et al. (2010). T values were assumed to be zero for the phytoplankton endmember since neither phytoplankton nor aquatic plants produce taraxerol.

For the terrestrial plant endmember, we applied a $\delta^{13}C$ value of $-27.4\pm0.8\%$, which was from terrestrial-derived POM in the southeast Amazon Estuary (Dittmar et al., 2001), and coincided

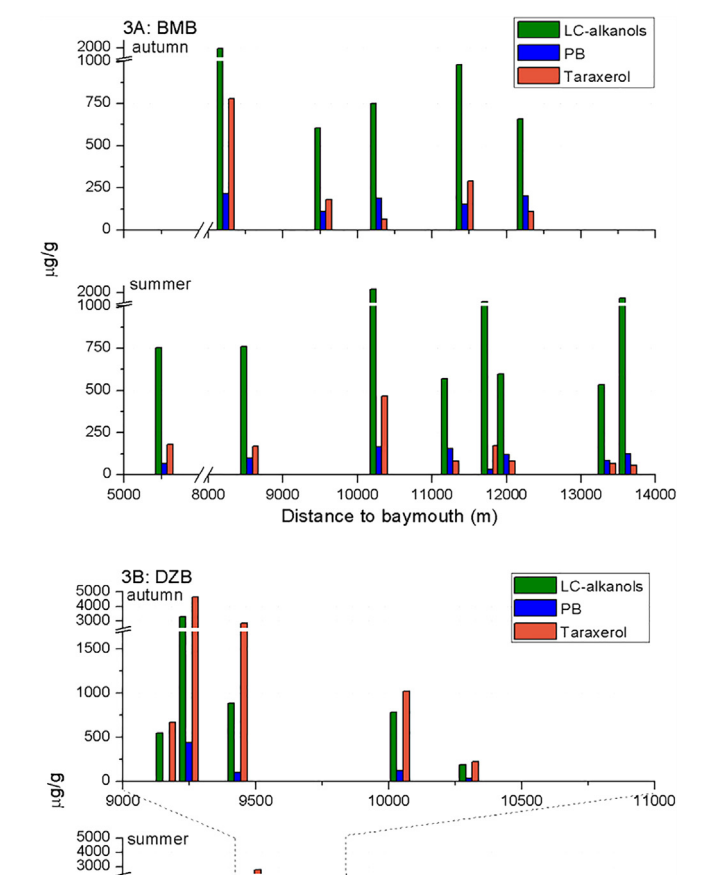


Fig. 3. Spatial distribution of C_{26} , C_{28} and C_{30} LC-alkanols, brassicasterol + dinosterol + $C_{37:2}$ and $C_{37:3}$ alkenones (PB), and taraxerol concentrations. 3A and 3B for BMB and DZB respectively. Sources of all lipid biomarkers are listed in Table 1. Autumn samples in DZB were collected within the distance indicated by the dashed lines.

10000 11000 12000 13000 14000

Distance to baymouth (m)

15000 16000

1500 1000

500

7000

8000

9000

with those of non-mangrove plants in BMB reported by Bao et al. (2013a). The terrestrial non-mangrove endmember value of T (=taraxerol/n-C₃₁ alkane) was assumed to be 0.05, which was the 'base level' of taraxerol relative to the n- C_{29} alkane proposed by Versteegh et al. (2004). Since the *n*-C₃₁ alkane was the most abundant alkane in our samples, as opposed to n-C₂₉ alkane in the study by Versteegh et al. (2004), our T values use $n-C_{31}$ alkane in the denominator rather than n- C_{29} . A T value of 0.05 accounts for the fact that taraxerol is also produced by several species of nonmangrove higher plants from the families Asteraceae, Betulaceae, Lauraceae (Versteegh et al., 2004), Rumitaceae (Beaton et al., 1955), Moraceae (Vilegas et al., 1997), Celastraceae (Cordeiro et al., 1999), and Euphorbiaceae (Setzer et al., 2000). Since there is no biomarker common to all mangroves that is not found in other vascular plants, and taraxerol is produced in exceptionally high abundance by Rhizophora spp. mangroves (e.g., 15.9 mg/g dry leaf; Versteegh et al., 2004) and L. racemosa (He et al., 2018), we estimated the fractional occurrence of Rhizophora and L. racemosa mangroves in both estuaries relative to other genera to derive an estimate of the OM contribution from all mangroves. In BMB, Rhizophora and L. racemosa are estimated to account for 24% of mangroves on average (from Guo et al., 2014). In DZB, *Rhizophora* occurrence averaged 50% (from Wu et al., 2016).

The significant difference between T values in the two bays may have been caused by the fact that leaf samples were collected from two different species of *Rhizophora* (R. apiculata in BMB and R. stylosa in DZB), since R. stylosa leaves in DZB had T values that were a factor of three greater than those from R. apiculata from BMB (Table 3). This was reflected in sedimentary T values that were a factor of 4–5 times greater in DZB than in BMB (Table 3). We therefore applied different endmember values for T in the two estuaries, 90 ± 32 for BMB and 280 ± 69 for DZB (Table 3). Notwithstanding the different T values in DZB and BMB, the ratio $T_{\rm sediment}/T_{\rm leaf}$ was comparable in the two estuaries within error (Table 3).

A mangrove $\delta^{13}C$ endmember value of $-29.1 \pm 1.2\%$ (n = 20) was adopted for both estuaries since there was no significant difference between the two locations (Table 2). $\delta^{13}C$ values of mangrove lipids increase by about 0.2% per ppt increase in salinity (Ladd and Sachs, 2013; Park et al., 2019; He et al., 2020), implying that the $\delta^{13}C$ values of sediment samples were likely influenced by both the source of the OM as well as the salinity.

3.4.2. Three-endmember mixing model based on $\delta^{13}C$ and T

The fractional contributions of terrestrial OM (f_{terr}), phytoplankton OM (f_{phyto}) and mangrove OM (f_{mang}) were estimated using $\delta^{13}C$ and T values (Table 4). In the mixing models, mangrove contribution was calculated by T values with normalization by the fraction occurrence of *Rhizophora* (and *L. racemosa* in BMB) among all mangroves. The results of three-endmember mixing model can be found in Fig. 5 and Table 5.

4. Discussion

4.1. Evaluation of OM sources

All proxies and mixing models were consistent in showing a greater contribution of higher plant OM relative to phytoplankton OM in the two estuaries. Average f_{terr} , f_{mang} , and f_{phyto} were $57 \pm 21\%$, $19 \pm 11\%$, $24 \pm 17\%$ (n = 13) in BMB and $40 \pm 19\%$, $15 \pm 16\%$, $45 \pm 22\%$ (n = 14) in DZB, respectively (Fig. 5, Table 5). High C/N values typical of mangrove sediments (Kristensen et al., 2008), together with low δ^{13} C values, suggest a significant input of plant litter to the subtidal sediments of BMB and DZB. With $CPI_{alk} > 1$, Paq < 0.3 and BIT > 0.6 (Fig. 4), river-delivered OM, including OM from both higher plants and in situ production in the rivers, is inferred to be the largest source of OM to subtidal sediments in both BMB and DZB. At most sites, fterr was the highest fraction, followed by f_{phyto} , and then f_{mang} . The sum of f_{terr} + f_{mang} , which averaged $82 \pm 8\%$ (autumn) and $73 \pm 20\%$ (summer) in BMB, as well as 66 ± 18% (autumn) in DZB, respectively, indicates that higher plant OM dominated the sedimentary OM reservoir.

The presence of mid-chain n-alkanes (i.e., n- C_{23} and n- C_{25} alkanes) in the sediments implies that non-emergent aquatic plants such as seagrasses (Ficken et al., 2000) contributed to the sedimentary OM. Stations without nearby mangroves (DZB summer-1, 2, 8, 9) had the highest Paq values (Supplementary Table S6), indicating greater input from aquatic macrophytes. In both BMB and DZB, narrow river channels may have prevented intensive OM exchange with the open estuary (Yun et al., 2017). Although tidal transport of seagrass OM is possible, we do not distinguish between aquatic OM derived from seagrasses and other macrophytes in the discussion below.

The majority of higher plant OM in surface subtidal sediments in both estuaries appears to have come from terrestrial non-mangrove plants rather than mangroves. In BMB, f_{terr} exceeded f_{mang} by 36% (absolute value and hereafter) in autumn samples

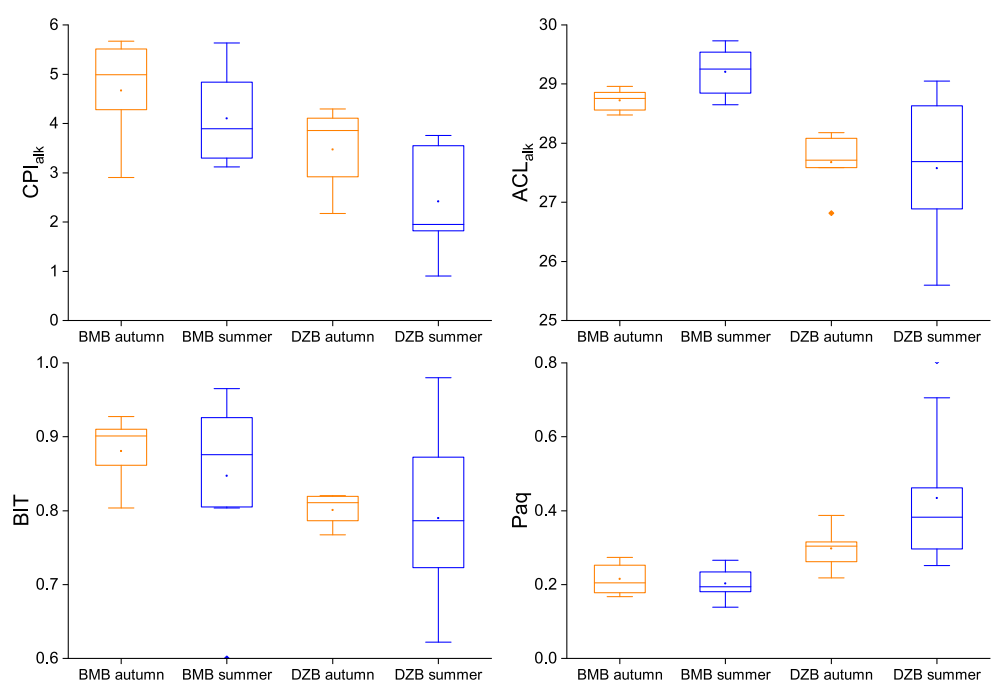


Fig. 4. Box chart of CPI_{alk}, Paq, BIT and ACL_{alk}.

Table 3 T (taraxerol/n- C_{31} alkane) values of surface sediments and *Rhizophora* leaf samples.

Station No.	Т	$\frac{T_{sediment}}{T_{leaf}}$	Taraxerol _{leaf} µg/g TOC _{(Rhizophora} apiculata)	T _{leaf} (Rhizophora apiculata)	Station No.	T	$\frac{T_{sediment}}{T_{leaf}}$	Taraxerol _{leaf} μg/g TOC (Rhizophora stylosa)	T _{leaf} (Rhizophora stylosa)
BMB autumn-1	1.65	1.83%	7815	44.4	DZB autumn-1	8.32	2.97%	11,634	194
BMB autumn-2	4.08	4.51%	9939	92.8	DZB autumn-2	16.9	6.03%	12,551	357
BMB autumn-3	0.99	1.10%	6169	112	DZB autumn-3	66.6	23.8%	6847	263
BMB autumn-4	3.19	3.53%	5094	112	DZB autumn-4	11.3	4.02%	5696	306
BMB autumn-5	10.2	11.3%			DZB autumn-5	6.58	2.35%		
BMB autumn	4.01 ± 3.65	4.45 ± 4.04%	7254 ± 2111	90.3 ± 31.9	DZB autumn	21.9 ± 25.3	7.93 ± 9.03%	9182 ± 3414	280 ± 69.1
avg. ± std					avg. ± std				
BMB summer-1	0.77	0.85%			DZB summer-1	0.00	0.00%		
BMB summer-2	1.40	1.55%			DZB summer-2	0.00	0.00%		
BMB summer-3	2.89	3.21%			DZB summer-3	3.64	1.30%		
BMB summer-4	1.60	1.77%			DZB summer-4	1.78	0.64%		
BMB summer-5	1.46	1.61%			DZB summer-5	25.3	9.02%		
BMB summer-6	4.03	4.47%			DZB summer-6	14.4	5.15%		
BMB summer-7	3.27	3.62%			DZB summer-7	75.7	27.0%		
BMB summer-8	4.40	4.87%			DZB summer-8	0.00	0.00%		
BMB summer avg. ± std	2.95 ± 1.36	2.74 ± 1.50%			DZB summer-9	12.8	4.56%		
-					DZB summer avg. ± std	32.0 ± 29.6	5.30 ± 8.72%		

and 39% in summer samples, with similar but somewhat less extreme proportions of 32% in autumn and 21% in summer for DZB sediments (Table 5). Although sedimentary taraxerol concentrations were high in surface sediments compared to other lipids (Table 3 and Supplementary Table S3), this does not necessarily imply a significant contribution of mangrove OM, as its abundance in *Rhizophora* mangrove leaves is very high. Indeed, the T values in surface sediments were much lower than those in leaf samples (Table 3), as expected since the n- C_{31} alkane is produced by most if not all higher plants including non-*Rhizophora* mangrove species (that don't produce taraxerol).

Although the T values from *Rhizophora* leaves in BMB and DZB were much higher than the taraxerol/n- C_{29} alkane values measured in the southeast Atlantic by Versteegh et al. (2004), the ratio

of $T_{\rm sediment}$ to $T_{\rm leaf}$ was generally small, implying that only about 5% (absolute percentage) of *Rhizophora* OM was incorporated into the surface subtidal sediments. Possible explanations are: (1) preferential incorporation of mangrove-derived OM into sub-surface sediments (Alongi, 2014), (2) downstream transport of mangrove OM rather than local burial, and/or (3) early diagenetic losses of taraxerol.

Indeed, previous studies reported a larger proportion of mangrove litter exported to the sea (Rajkaran and Adams, 2007; Adame and Lovelock, 2011) rather than decomposed in situ (Duarte and Cebrian, 1996; Bouillon et al., 2008b). The positive correlation between f_{mang} and salinity may result from the latter process (Table 5). It is therefore possible that high current velocities and slow incorporation of mangrove OM into sediments resulted

Table 4 Endmember values in 3-endmember mixing model.

	Aquatic phytoplankton	Terrestrial plants	Mangroves	Rhizohpora occurrence (f_{Rhi}/f_{mang})
δ ¹³ C (‰)	-20.8 ± 0.4	-27.4 ± 0.8	-29.1 ± 1.2	24% for BMB
T	0	0.05	90 ± 32 for BMB	50% for DZB
			280 ± 69 for DZB	
Equations				
$\delta^{13}C_{\text{sample}} = \delta^{13}C_{\text{t}}$	$_{\text{terr}} * f_{\text{terr}} + \delta^{13}C_{\text{mang}} * f_{\text{mang}} + \delta^{13}C_{\text{phyto}} * f_{\text{phyto}}$	hyto		
	* $(f_{terr} + f_{mang} - f_{Rhi.}) + T_{Rhi.}$ * $f_{Rhi.}$			
$f_{Rhi.}/f_{mang} = 0.2$	24 (BMB) or 0.50 (DZB)			
$f_{terr} + f_{mang} + f$	c _{phyto} = 1			
	v_{to} and f_{Rhi} refer to fraction of terrestria	OM OM	1 1, 01, 101; 1 1	. 1014

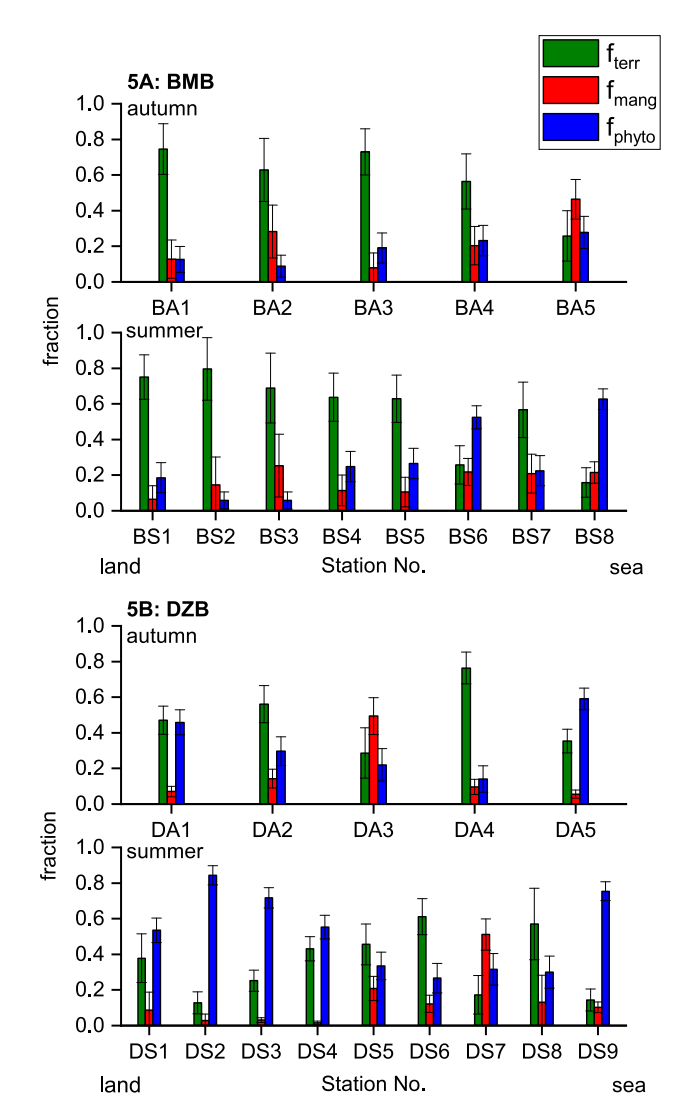


Fig. 5. Three-endmember calculation using $\delta^{13}\text{C}$ and T values. 5A and 5B are for BMB and DZB, respectively.

in mangrove-OM deficiency in sediments even at sites proximal to mangrove trees.

Kumar et al. (2019) assessed the sedimentary diagenesis of triterpenoids in mangrove intertidal sediments from the Potengi estuary in northeast Brazil, where highly abundant taraxerol acetate, together with the absence of taraxerol, suggested an early diagenetic alteration of mangrove-derived OM. He et al. (2018) observed much lower abundances of taraxerol degradation products relative to intact taraxerol in sediments from the Shark River

estuary in Florida, USA, but noted that they were also present in fresh mangrove leaves and suggested they may result from photochemical or microbial processes occurring very early in the diagenetic process. Without measurements of taraxerone, taraxerol acetate and other known taraxerol degradation products we are unable to quantify the fraction of taraxerol in sediments that may have undergone diagenesis. Assuming some diagenetic loss of taraxerol occurred, our estimates of mangrove-derived OM based solely on taraxerol abundance are necessarily underestimates.

That said, there is circumstantial evidence that the OM in BMB and DZB sediments underwent relatively minor diagenetic alteration. In contrast to the results of Kumar et al. (2019) where taraxerol itself was not detected in the surface sediments, the taraxerol concentrations in our sediment samples were high (1160 µg/g TOC in DZB and 207 µg/g TOC in BMB). In addition, the homologous distribution of n-alkyl lipids (i.e., n-alkanes, nalkanols and n-FAs), which had a high odd/even (n-alkanes, $CPI_{26-33} = 4.3 \pm 1.0$, n = 13, in BMB and 2.8 ± 1.1 , n = 14, in DZB) or even/odd (n-alkanols $CPI_{21-30} = 7.1 \pm 3.5$ in BMB and 3.2 ± 2.9 in DZB) predominance imply limited diagenetic alteration of the sedimentary OM. This contrasts with the results from Kumar et al. (2019), where a less strong odd/even predominance (e.g., high concentration of n- C_{28} alkane and its derivatives) was observed for nalkanes in the sediments. Nevertheless, a high concentration of n- C_{25} FA in DZB sediments, that did not coincide with high n- C_{25} alkane or alkanol concentrations, may suggest diagenesis, or more likely, an additional source of this *n*-FA. We also note that preliminary results of ²¹⁰Pb analysis of sediment cores suggests either very high accumulation rates or strong vertical mixing (e.g., bioturbation), since there was no systematic variation of ²¹⁰Pb activities in cores collected from BMB or DZB (Supplementary Fig. S4).

Despite the fact that taraxerol is source-specific and well preserved in sediments, it is only produced by two genera of mangroves. While the Rhizophora spp. is a very common and widespread genus, it is not the only mangrove species present in most mangrove systems, and its fractional occurrence can vary with salinity, potentially biasing results. Therefore, the estimation of mangrove contributions to sedimentary OM from taraxerol concentrations will be sensitive to the assemblage of mangroves present in each estuary and sampling location, which in this study was not well constrained. Rather than being able to quantify the OM contribution to these estuarine sediments from all mangroves. we are left with having to quantify only the mangrove OM that came from Rhizophora (and L. racemosa in BMB). Though this approach is not ideal, we note that Rhizophora mangroves are both dominant and widespread in the two estuaries, so this approach remains one of the few direct means apart from pollen of tracking mangrove OM contributions to sediments. The assemblage of mangrove species also has an important influence on the deposition of OM in mangrove forests (Bouillon et al., 2008a; Adame and

 Table 5

 Results of 3-endmember mixing model. The range of sedimentary OM contributed by mangroves was estimated from taraxerol concentrations by assuming an average of fractional abundances of *Rhizophora* spp. to the total mangrove assemblage. The resulting contributions of OM from terrestrial non-mangrove plants (f_{terr}), mangroves (f_{mang}) and phytoplankton (f_{phyto}) is shown.

Station No.	f _{terr} ± std (%)	$f_{mang} \pm std$ (%)	$f_{phyto} \pm std$ (%)	Station No.	f _{terr} ± std (%)	$f_{mang} \pm std$ (%)	f _{phyto} ± std (%)
BMB autumn-1	75 ± 14	13 ± 11	13 ± 7	DZB autumn-1	47 ± 8	7 ± 3	46 ± 7
BMB autumn-2	63 ± 18	28 ± 15	9 ± 6	DZB autumn-2	56 ± 10	14 ± 5	30 ± 8
BMB autumn-3	73 ± 13	8 ± 8	19 ± 8	DZB autumn-3	29 ± 14	49 ± 10	22 ± 9
BMB autumn-4	56 ± 15	20 ± 11	23 ± 8	DZB autumn-4	76 ± 9	10 ± 4	14 ± 7
BMB autumn-5	26 ± 14	46 ± 11	28 ± 9	DZB autumn-5	35 ± 7	6 ± 2	59 ± 6
Pearson Corr. with salinity	-0.97	0.86	0.79	Pearson Corr. with salinity	0.00	-0.39	0.39
BMB summer-1	75 ± 12	6 ± 8	19 ± 8	DZB summer-1	38 ± 14	9 ± 10	53 ± 7
BMB summer-2	80 ± 17	15 ± 16	6 ± 5	DZB summer-2	13 ± 6	3 ± 4	84 ± 5
BMB summer-3	69 ± 20	25 ± 18	6 ± 5	DZB summer-3	25 ± 6	3 ± 1	72 ± 6
BMB summer-4	64 ± 14	11 ± 9	25 ± 9	DZB summer-4	43 ± 7	2 ± 1	55 ± 7
BMB summer-5	63 ± 13	11 ± 8	27 ± 9	DZB summer-5	46 ± 11	21 ± 7	34 ± 8
BMB summer-6	26 ± 11	22 ± 8	52 ± 6	DZB summer-6	61 ± 10	12 ± 5	27 ± 8
BMB summer-7	57 ± 16	21 ± 11	22 ± 8	DZB summer-7	17 ± 11	51 ± 9	32 ± 9
BMB summer-8	16 ± 8	21 ± 6	63 ± 6	DZB summer-8	57 ± 20	13 ± 15	30 ± 9
Pearson Corr. with salinity	-0.84	0.56	0.76	DZB summer-9	14 ± 6	10 ± 3	75 ± 5
				Pearson Corr. with salinity	0.13	0.65	-0.56

Lovelock, 2011). The fact that f_{mang} was positively correlated with salinity may have been caused by either (or both) the fact that *Rhizophora* spp. may increase in abundance as salinity increases or that mangrove OM, including that from *Rhizophora* spp., may be preferentially transported downstream. Because the available information on *Rhizophora* spp. occurrence in the two estuaries indicates that this genus is widespread throughout both BMB (Nong et al., 2011) and DZB (Wu et al., 2016) we suggest the latter may be the more likely explanation, but cannot rule out the former without additional *Rhizophora* distribution data.

A potentially large uncertainty in the estimation of different OM sources with the three-endmember mixing model is that it does not account for OM derived from seagrass which tends to grow below the intertidal zone of mangrove habitats (Gonneea et al., 2004). Although seagrasses have been reported in the BMB estuary (Gao et al., 2018) they are not thought to be a large source of OM to sediments near mangrove-fringed regions of BMB (Bao et al., 2013a). DZB is not recognized as a major location of seagrass beds on Hainan Island. To the best of our knowledge, only one study by Jiang et al. (2017) mentioned seagrass occurrence in DZB (location not specified). An effort was made to estimate the potential OM contribution from seagrass by measuring the abundance of α,β dihydroxy fatty acid, which is biomarker for Zostera seagrass (de Leeuw et al., 1995), but none was detected in the most inland samples from each estuary. In addition, n-C₂₂ alkanol, which was presumed to be seagrass-derived by Volkman et al (2008), was not abundant in our samples. It is possible that these lipids are either not produced in high abundance by seagrasses common to the Hainan Island estuaries we studied, or that it is poorly preserved in sediments.

4.2. Comparisons between BMB and DZB

The significant difference in TOC values between the two estuaries (p < 0.005) was likely due to sediment grain size differences. Preliminary results of grain size analysis of two sediment cores collected from the studied estuaries showed that the TOC content of sediments was negatively correlated with their median grain size, which were 149 μm in BMB and 179 μm DZB, respectively (Supplementary Fig. S5). Because sandy sediments generally retain less OM than muddy or silty sediments (Hemingway et al., 2019), the different TOC concentrations do not necessarily imply less OM input in DZB, but rather poorer preservation. Most of the DZB summer sediment had extremely low TN, suggesting either that sediments in those stations were highly degraded, with fresh

mangrove OM largely consumed or exported, or the sandy nature of the sediment resulted in TN (and TOC) concentrations that were below our detection limit (Table 2). A previous study by Xin et al. (2014) also suggested that BMB had higher carbon storage than DZB. OM preservation in BMB, which generally had siltier sediments than DZB, likely exceeded that in the largely sandy sediments of DZB. However, the rinsing procedure prior to the TOC analysis likely removed part of the soluble OC, which would lead to an underestimation of TOC, especially in DZB where the wt% organic carbon contents were low.

Compared to DZB, BMB sediments receive a greater relative proportion of OM from terrestrial plants and a smaller relative proportion from phytoplankton. BMB samples were more $^{13}\text{C}\text{-enriched}$ (Table 2), which could be explained by a greater contribution of OM to BMB sediments from more $^{13}\text{C}\text{-enriched}$ sources such as vascular plants. The ACLalk, CPlalk, and BIT values in BMB samples were all higher than in DZB samples, while Paq values were lower. Values 17% higher for f_{terr} and 21% lower for f_{phyto} (by absolute values) in BMB samples were also consistent with the former indices. The higher $T_{\text{sediment}}/T_{\text{leaf}}$ in DZB (Table 3) is attributable to a greater contribution of *Rhizophora* OM, albeit the total mangrove OM proportion was not statistically different between BMB and DZB.

OM sedimentation and exchange in mangrove forests are largely controlled by geomorphological features and hydrology including river discharge, tidal amplitude and rainfall, which can vary widely over small spatial scales (Mao et al., 2006; Lee, 2015; Signa et al., 2017). One possibility is that the drier climate in western Hainan resulted in sparser terrestrial vegetation coverage, and correspondingly less plant-derived OM delivery to DZB sediments. Another possibility is that microbes may preferentially consume aquatic OM rather than mangrove OM when TOC concentrations are low (e.g., < 1%, Bouillon and Boschker, 2006). Among all 14 samples collected in DZB, only two of them had TOC values > 1%. Therefore, in addition to more phytoplankton OM input to DZB, the higher lability of this OM likely results in it being consumed more quickly than OM derived from mangroves.

4.3. Temporal variations

Because the sampling was not carried out at exactly the same locations during summer and autumn we limit the comparison of seasonal changes in sedimentary OM apportionment to sites located within 1.5 km of each other, thus eliminating sites BMB summer-8 and DZB summer-1, 2, 3, 4 from this part of the discussion. There was no apparent seasonal difference in OM sources

based on our three-endmember mixing model, a possible consequence of a small sample set. Nevertheless, a shift in the relative abundance of different *n*-alkane chain lengths in DZB did imply a likely change in OM sources from the wet season to the dry season. Since the most abundant n-alkane in mangrove leaves was n- C_{31} alkane, it is possible that mangrove OM contributions to DZB sediments were higher in autumn than in summer, but that the uncertainties associated with endmember values in our model do not reveal such a shift. This is further supported by higher CPI_{alk} and lower Paq values in autumn samples than summer samples in DZB. One possible explanation for the lower mangrove OM contribution to the sediment in summer than in autumn is the time delay between the growth of leaves in the wet season, and their abscission during the dry season. For example, in southern Hainan Island, maximum litter fall occurred during November and the minimum occurred in May, with no association with extreme weather (Zhang and Chen. 2003). Secondly, mangrove crabs can greatly influence the mobilization of mangrove litter (Twilley et al., 1997; Rajkaran and Adams, 2007). Reduced mangrove crab activity in autumn was shown in one study to reduce the mobilization of litter and increase in situ accumulation of mangrovederived OM (Bouillon et al., 2008b).

4.4. Implications for carbon accumulation in mangrove-fringed estuaries

Mangrove swamps represent one of the most efficient global sinks for carbon, with mangrove, seagrass, and tidal marsh sediments representing 50% of all C sequestered in marine sediments (Macreadie et al., 2019). Preliminary results of ¹³⁷Cs dating of sediment cores collected from the two studied estuaries indicate that at least the upper 48 cm in BMB and 74 cm in DZB were deposited during the last 50 years. Considering the average values of TOC (2.5% in BMB and 0.5% in DZB), bulk density (1.4 g/cm³ in both estuaries), and f_{mang} (avg. 18%), the mangrove carbon storage would be in a range of 0.1 g/cm² (DZB) to 0.3 g/cm² (BMB). According to Zhang and Sui (2001), the total coverage of mangrove reserves in SE China in 1997 was 14,877 hm². Based on these estimates, the minimum carbon sequestration rate of mangrove systems in SE China during the last 50 years would be 0.15-0.47 Tg C/yr, or 0.6%-2% of global carbon sequestration in mangrove systems (24 Tg C/yr, estimated by Alongi (2014)).

5. Conclusions

Sedimentary OM sources were quantified during two seasons in two estuaries located in northwest and northeast Hainan Island using lipid biomarkers and stable carbon isotopes. The primary OM sources in both BMB and DZB were, in decreasing order of significance, terrestrial higher plants (40–57%), phytoplankton (24–45%), and mangroves (15–19%). Albeit not the major OM source, mangrove systems in SE China are estimated to contribute at least 0.6–2% of global carbon sequestration in mangrove systems.

A three-endmember mixing model based on carbon isotopes, and the concentrations of n- C_{31} alkane and taraxerol reveals that subtidal sediments in BMB, which receives 29% more rainfall annually than DZB, accumulate a 10–21% higher proportion (by absolute value) of terrestrial plant OM than DZB, with the phytoplankton OM fraction 16–24% higher in DZB.

The proportion of sedimentary OM derived from mangroves and phytoplankton increased seaward in both estuaries. The proportional increase in mangrove OM is attributed to its relatively refractory nature and transport from upstream locations where it is produced, as well as the potential change of mangrove commu-

nity structure, with the fraction of *Rhizophora* spp. increasing seaward.

On a seasonal basis, lipid biomarker concentrations indicated that the subtidal sediments in summer contained a slightly lower proportion of mangrove OM. This may have resulted from more effective leaf litter transport offshore during the wet season and more extensive leaf abscission during the dry season.

Future studies using this approach to apportion sedimentary OM sources in mangrove-containing estuarine systems should attempt to better constrain its limitations and would therefore benefit from: (1) quantitative estimates of the mangrove assemblage, (2) comprehensive measurements of the T (taraxerol/n-C₃₁ alkane) index in the local plant community, and (3) quantification of taraxerol degradation products in sediments.

Declaration of Competing Interest

The authors declare that they have no known competing financial interests or personal relationships that could have appeared to influence the work reported in this paper.

Acknowledgements

We are grateful to Wenqing Wang, Guanghui Lin and Youshao Wang for suggestions on mangrove sampling, to Zicheng Wang for help with field work, to Li Li and Pengfei Hou for technical help. We thank the constructive suggestions made by two anonymous reviewers which greatly improved this manuscript. We also thank Co-Editor-in-Chief Dr. John Volkman and Associate Editor Dr. Stefan Schouten for their constructive comments. This work was supported by the National Key Research and Development Program of China (MZ; Grant No. 2016YFA0601403), the National Natural Science Foundation of China (U1706219, 41630966), and the "111" Project (B13030). This is MCTL contribution #219.

Appendix A. Supplementary material

Supplementary data to this article can be found online at https://doi.org/10.1016/j.orggeochem.2020.104066.

Associate Editor—S. Schouten

References

Adame, M.F., Lovelock, C.E., 2011. Carbon and nutrient exchange of mangrove forests with the coastal ocean. Hydrobiologia 663, 23–50.

Alongi, D., 1994ab. Zonation and seasonality of benthic primary production and community respiration in tropical mangrove forests. Oecologia 98, 320–327.
Alongi, D. 2014. Cashop, regime and storage in panagroup forests. Appual Business.

Alongi, D.M., 2014. Carbon cycling and storage in mangrove forests. Annual Review of Marine Science 6, 195–219.

Atwood, T.B., Connolly, R.M., Almahasheer, H., Carnell, P.E., Duarte, C.M., Ewers Lewis, C.J., Irigoien, X., Kelleway, J.J., Lavery, P.S., Macreadie, P.I., 2017. Global patterns in mangrove soil carbon stocks and losses. Nature Climate Change 7, 523–528.

Bao, H., Wu, Y., Tian, L., Zhang, J., Zhang, G., 2013a. Sources and distributions of terrigenous organic matter in a mangrove fringed small tropical estuary in South China. Acta Oceanologica Sinica 32, 18–26.

Bao, H., Wu, Y., Unger, D., Du, J., Herbeck, L.S., Zhang, J., 2013b. Impact of the conversion of mangroves into aquaculture ponds on the sedimentary organic matter composition in a tidal flat estuary (Hainan Island, China). Continental Shelf Research 57, 82–91.

Beaton, J.M., Spring, F.S., Stevenson, R., Steward, J.L., 1955. Triterpenoids XXXVII. The constitution of taraxerol. Journal of America Chemistry Society, 2131–2137.

Bosch, C., Andersson, A., Kruså, M., Bandh, C., Hovorkova, I., Klanova, J., Knowles, T.D. J., Pancost, R.D., Evershed, R.P., Gustafsson, O., 2015. Source apportionment of polycyclic aromatic hydrocarbons in central European soils with compound-specific triple isotopes (δ¹3C, Δ¹4C, and δ²H). Environmental Science and Technology 49, 7657–7665.

Bouillon, S., Boschker, H.T.S., 2006. Bacterial carbon sources in coastal sediments: a cross-system analysis based on stable isotope data of biomarkers. Biogeosciences 3, 175–185.

- Bouillon, S., Moens, T., Dehairs, F., 2004. Carbon sources supporting benthic mineralization in mangrove and adjacent seagrass sediments (Gazi Bay, Kenya). Biogeosciences 1, 71–78.
- Bouillon, S., Borges, A.V., Castaneda-Moya, E., Diele, K., Dittmar, T., Duke, N.C., Kristensen, E., Lee, S.Y., Marchand, C., Middelburg, J.J., Rivera-Monroy, V.H., Smith III, T.J., Twilley, R.R., 2008a. Mangrove production and carbon sinks: A revision of global budget estimates. Global Biogeochemical Cycles 22, 1–12.
- Bouillon, S., Connolly, R.M., Lee, S.Y., 2008b. Organic matter exchange and cycling in mangrove ecosystems: Recent insights from stable isotope studies. Journal of Sea Research 59, 44–58.
- Carreira, R.S., Cordeiro, L.G.M.S., Bernardes, M.C., Hatje, V., 2016. Distribution and characterization of organic matter using lipid biomarkers: A case study in a pristine tropical bay in NE Brazil. Estuarine Coastal and Shelf Science 168, 1–9.
- Chen, G., Chen, G., 1998. Analysis of the mangrove flora in China. Ecologicence 17, 19–23 (in Chinese with English abstract).
- Chen, M., Chen, S., Chen, C., Chen, X., Cai, Z., Wu, Z., Zhang, G., Yao, H., 2017. Studies on protection and sustainable utilization of lagoon resource around Hainan Island. Transactions of Oceanology and Limnology, 107–114 (in Chinese with English abstract).
- Cordeiro, P.J.M., Vilegas, J.H.Y., Lanças, F.M., 1999. HRGC-MS analysis of terpenoids from *Maytenus ilicifolia* and *Maytenus aquifolium* ("Espinheira Santa"). Journal of the Brazilian Chemical Society 10, 523–526.
- Cranwell, P.A., Eglinton, G., Robinson, N., 1987. Lipids of aquatic organisms as potential contributors to lacustrine sediments—II. Organic Geochemistry 11, 513–527.
- Dale, N.G., 1974. Bacteria in intertidal sediments: Factors related to their distribution. Limnology and Oceanography 19, 509–518.
- de Leeuw, J.W., Rijpstra, W.I.C., Nienhuis, P., 1995. Free and bound fatty acids and hydroxy fatty acids in the living and decomposing eelgrass *Zostera marina* L. Organic Geochemistry 23, 721–728.
- Dittmar, T., Lara, R.J., Kattner, G., 2001. River or mangrove? Tracing major organic matter sources in tropical Brazilian coastal waters. Marine Chemistry 73, 253–271
- Duarte, C.M., Cebrian, J., 1996. The fate of marine autotrophic production. Limnology and Oceanography 41, 1758–1766.
- Eglinton, G., Hamilton, R.J., 1967. Leaf epicuticular waxes. Science 156, 1322–1335. Ficken, K.J., Li, B., Swain, D.L., Eglinton, G., 2000. An *n*-alkane proxy for the sedimentary input of submerged/floating freshwater aquatic macrophytes. Organic Geochemistry 31, 745–749.
- França, M.C., Francisquini, M.I., Cohen, M.C.L., Pessenda, L.C.R., Rossetti, D.F., Guimarães, J.T.F., Smith, C.B., 2012. The last mangroves of Marajó Island Eastern Amazon: Impact of climate and/or relative sea-level changes. Review of Palaeobotany and Palynology 187, 50–65.
- Gao, T., Ding, D., Guan, W., Liao, B., 2018. Carbon stocks of coastal wetland ecosystems on Hainan Island, China. Polish Journal of Environmental Studies 27, 1061–1069.
- Gonneea, M.E., Paytan, A., Herrera-Silveira, J.A., 2004. Tracing organic matter sources and carbon burial in mangrove sediments over the past 160 years. Estuarine, Coastal and Shelf Science 61, 211–227.
- Guo, J., Qin, Y., Zhu, Y., Guo, Z., Wu, G., 2014. Correlation between mangrove species distribution and soil environmental factors at Qinglan Harbour, Hainan Province, China. Forest Research 27, 149–157 (in Chinese with English abstract).
- Hamilton, S.E., Friess, D.A., 2018. Global carbon stocks and potential emissions due to mangrove deforestation from 2000 to 2012. Nature Climate Change 8, 240–244.
- He, B., Dai, M., Huang, W., Liu, Q., Chen, H., Xu, L., 2010. Sources and accumulation of organic carbon in the Pearl River Estuary surface sediment as indicated by elemental, stable carbon isotopic, and carbohydrate compositions. Biogeosciences 7, 3343–3362.
- He, D., Mead, R.N., Belicka, L., Pisani, O., Jaffé, R., 2014. Assessing source contributions to particulate organic matter in a subtropical estuary: A biomarker approach. Organic Geochemistry 75, 129–139.
- He, D., Rivera-Monroy, V.H., Jaffe, R., Zhao, X., 2020. Mangrove leaf species-specific isotopic signatures along a salinity and phosphorus soil fertility gradients in a subtropical estuary. Estuarine, Coastal and Shelf Science 106768.
- He, D., Simoneit, B., Cloutier, J., Jaffe, R., 2018. Early diagenesis of triterpenoids derived from mangroves in a subtropical estuary. Organic Geochemistry 125, 196–211.
- Hemingway, J.D., Rothman, D.H., Grant, K.E., Rosengard, S.Z., Eglinton, T.I., Derry, L. A., Galy, V.V., 2019. Mineral protection regulates long-term global preservation of natural organic carbon. Nature 570, 228–231.
- Hopmans, E.C., Weijers, J.W.H., Schefuß, E., Herfort, L., Sinninghe Damsté, J.S., Schouten, S., 2004. A novel proxy for terrestrial organic matter in sediments based on branched and isoprenoid tetraether lipids. Earth and Planetary Science Letters 224, 107–116.
- Jaffé, R., Mead, R., Hernandez, M.E., Peralba, M.C., Diguida, O.A., 2001. Origin and transport of sedimentary organic matter in two subtropical estuaries: a comparative, biomarker-based study. Organic Geochemistry 32, 507–526.
- Jennerjahn, T.C., Ittekkot, V., 2002. Relevance of mangroves for the production and deposition of organic matter along tropical continental margins. Naturwissenschaften 89, 23–30.
- Jiang, Z., Liu, S., Zhang, J., Zhao, C., Wu, Y., Yu, S., Zhang, X., Huang, C., Huang, X., Kumar, M., 2017. Newly discovered seagrass beds and their potential for blue carbon in the coastal seas of Hainan Island, South China Sea. Marine Pollution Bulletin 125, 513–521.

- Kennedy, H., Gacia, E., Kennedy, D.P., Papadimitriou, S., Duarte, C.M., 2004. Organic carbon sources to SE Asian coastal sediments. Estuarine Coastal and Shelf Science 60, 59–68.
- Killops, S.D., Frewin, N.L., 1994. Triterpenoid diagenesis and cuticular preservation. Organic Geochemistry 21, 1193–1209.
- Koch, B.P., Filho, P.W.M.S., Behling, H., Cohen, M.C.L., Kattner, G., Rullkötter, J., Scholz-Böttcher, B., Lara, R.J., 2012. Triterpenols in mangrove sediments as a proxy for organic matter derived from the red mangrove (*Rhizophora mangle*). Organic Geochemistry 42, 62–73.
- Kristensen, E., Bouillon, S., Dittmar, T., Marchand, C., 2008. Organic carbon dynamics in mangrove ecosystems: A review. Aquatic Botany 89, 201–219.
- Kumar, M., Boski, T., Lima-Filho, F., Bezerra, F., Vila, F., Bhuiyan, M.K.A., González-Pérez, J., 2019. Biomarkers as indicators of sedimentary organic matter sources and early diagenetic transformation of pentacyclic triterpenoids in a tropical mangrove ecosystem. Estuarine, Coastal and Shelf Science 229, 106403.
- Ladd, S.N., Sachs, J.P., 2013. Positive correlation between salinity and n-alkane δ^{13} C values in the mangrove *Avicennia marina*. Organic Geochemistry 64, 1–8.
- Lee, S.Y., 1995. Mangrove outwelling: a review. Hydrobiologia 295, 203-212.
- Lee, S.Y., 2015. Tropical mangrove ecology: Physical and biotic factors influencing ecosystem structure and function. Austral Ecology 24, 355–366.
- Li, M.S., Lee, S.Y., 1996. Mangroves of China: a brief review. Forest Ecology and Management 96, 241–259.
- Liao, B., Zheng, D., Zheng, S., Chen, Y., Song, X., 2000. The characteristics of species diversity for the successional series of mangrove community in Qinglan Harbor of Hainan Island. Ecologic Science 19, 17–22 (in Chinese with English abstract).
- Lugendo, B.R., Nagelkerken, I., Kruitwagen, G., Velde, G.V.D., Mgaya, Y.D., 2007. Relative importance of mangroves as feeding habitats for fishes: a comparison between mangrove habitats with different settings. Bulletin of Marine Science 80, 497–512.
- Macreadie, P.I., Anton, A., Raven, J.A., Beaumont, N., Connolly, R.M., Friess, D.A., Kelleway, J.J., Kennedy, H., Kuwae, T., Lavery, P.S., Lovelock, C.E., Smale, D.A., Apostolaki, E.T., Atwood, T.B., Baldock, J., Bianchi, T.S., Chmura, G.L., Eyre, B.D., Fourqurean, J.W., Hall-Spencer, J.M., Huxham, M., Hendriks, I.E., Krause-Jensen, D., Laffoley, D., Luisetti, T., Marbà, N., Masque, P., McGlathery, K.J., Megonigal, J. P., Murdiyarso, D., Russell, B.D., Santos, R., Serrano, O., Silliman, B.R., Watanabe, K., Duarte, C.M., 2019. The future of Blue Carbon science. Nature Communications 10, 3998.
- Mao, L., Zhang, Y., Bi, H., 2006. Modern pollen deposits in coastal mangrove swamps from northern Hainan Island, China. Journal of Coastal Research 22, 1423–1436.
- McLeod, E., Chmura, G.L., Bouillon, S., Salm, R., Bjork, M., Duarte, C.M., Lovelock, C.E., Schlesinger, W.H., Silliman, B.R., 2011. A blueprint for blue carbon: toward an improved understanding of the role of vegetated coastal habitats in sequestering CO₂. Frontiers in Ecology and the Environment 9, 552–560.
- Meng, X., Xia, P., Li, Z., Meng, D., 2017. Mangrove development and its response to Asian Monsoon in the Yingluo Bay (SW China) over the last 2000 years. Estuaries and Coasts 40, 540–552.
- Meyers, P.A., 1997. Organic geochemical proxies of paleoceanographic, paleolimnologic, and paleoclimatic processes. Organic Geochemistry 27, 213–250.
- Meziane, T., Tsuchiya, M., 2000. Fatty acids as tracers of organic matter in the sediments and food web of a mangrove/intertidal flat ecosystem, Okinawa, Japan. Marine Ecology Progress Series 200, 49–57.
- Nong, S., Yang, X., Li, D., Yang, L., Xu, Z., Chen, Y., Luo, Z., 2011. Vegetation composition in the mangrove forest Nature Protection Area of Qinglan, China. Plant Science Journal 29, 459–466 (in Chinese with English abstract).
- Park, J.W., Ladd, S.N., Sachs, J.P., 2019. Hydrogen and carbon isotope responses to salinity in greenhouse-cultivated mangroves. Organic Geochemistry 132, 23–36.
- Pisani, O., Orosb, D.R., Oyo-Ita, O.E., Ekpo, B.O., Jaffé, R., Simoneit, B.R.T., 2013. Biomarkers in surface sediments from the Cross River and estuary system, SE Nigeria: Assessment of organic matter sources of natural and anthropogenic origins. Applied Geochemistry 31, 239–250.
- origins. Applied Geochemistry 31, 239–250.

 Poynter, J.G., Eglinton, G., 1990. Molecular composition of three sediments from hole 717C. The Bengal Fan. Proceedings of the Ocean Drilling Program Scientific Results 116. 155–161.
- Prasad, M.B.K., Ramanathan, A.L., 2009. Organic matter characterization in a tropical estuarine-mangrove ecosystem of India: Preliminary assessment by using stable isotopes and lignin phenols. Estuarine Coastal and Shelf Science 84, 617–624.
- Prasad, M.B.K., Kumar, A., Ramanathan, A.L., Datta, D.K., 2017. Sources and dynamics of sedimentary organic matter in Sundarban mangrove estuary from Indo-Gangetic delta. Ecological Processes 6, 8.
- Rajkaran, A., Adams, J.B., 2007. Mangrove litter production and organic carbon pools in the Mngazana Estuary, South Africa. African Journal of Aquatic Science 32, 17–25.
- Requejo, A.G., Brown, J.S., Boehm, P.D., 1986. Lignin geochemistry of sediments from the Narragansett Bay Estuary. Geochimica et Cosmochimica Acta 50, 2707–2717.
- Resmi, P., Manju, M.N., Gireeshkumar, T.R., Kumar, C.S.R., Chandramohanakumar, N., 2016. Source characterisation of Sedimentary organic matter in mangrove ecosystems of northern Kerala, India: Inferences from bulk characterisation and hydrocarbon biomarkers. Regional Studies in Marine Science 7, 43–54.
- Setzer, W.N., Shen, X., Bates, R.B., Burns, J.R., Mcclure, K.J., Zhang, P., Moriarity, D.M., Lawton, R.O., 2000. A phytochemical investigation of *Alchornea latifolia*. Fitoterapia 71, 195–198.

- Signa, G., Mazzola, A., Kairo, J., Vizzini, S., 2017. Small scale variability of geomorphological settings influences mangrove-derived organic matter export in a tropical bay. Biogeosciences 14, 617–629.
- Thimdee, W., Deein, G., Sangrungruang, C., Nishioka, J., Matsunaga, K., 2003. Sources and fate of organic matter in Khung Krabaen Bay (Thailand) as traced by δ^{13} C and C/N atomic ratios and C/N atomic ratios. Wetlands 23, 729–738.
- Tue, N.T., Quy, T.D., Hamaoka, H., Mai, T.N., Omori, K., 2012. Sources and exchange of particulate organic matter in an estuarine mangrove ecosystem of Xuan Thuy National Park, Vietnam. Estuaries and Coasts 35, 1060–1068.
- Twilley, R.R., Pozo, M., Garcia, V.H., Rivera-Monroy, V.H., Zambrano, R., Bodero, A., 1997. Litter dynamics in riverine mangrove forests in the Guayas River estuary, Ecuador. Oecologia 111, 109–122.
- Versteegh, G.J.M., Schefuß, E., Dupont, L., Marret, F., Sinninghe Damsté, J.S., Jansen, J. H.F., 2004. Taraxerol and *Rhizophora* pollen as proxies for tracking past mangrove ecosystems. Geochimica et Cosmochimica Acta 68, 411–422.
- Vilegas, J.H.Y., Lanças, F.M., Vilegas, W., Pozetti, G.L., 1997. Further triterpenes, teroids and fucocoumarins from Brazilian medicinal plants of *Dorstenia* genus (Moraceae). Journal of the Brazilian Chemical Society, 85, 529–535.
- Volkman, J.K., Revill, A.T., Bonham, P.I., Clementson, L.A., 2007. Sources of organic matter in sediments from the Ord River in tropical northern Australia. Organic Geochemistry 38, 1039–1060.
- Volkman, J.K., Revill, A.T., Holdsworth, D.G., Fredericks, D., 2008. Organic matter sources in an enclosed coastal inlet assessed using lipid biomarkers and stable isotopes. Organic Geochemistry 39, 689–710.
- Volkman J.K., Smittenberg R.H., 2017. Lipid biomarkers as organic geochemical proxies for the paleoenvironmental reconstruction of estuarine environments. In: Weckström, K., Saunders, K., Gell, P., Skilbeck, C. (Eds), Applications of

- Paleoenvironmental Techniques in Estuarine Studies. Developments in Paleoenvironmental Research, vol. 20. Springer, Dordrecht.
- Wang, Y., Duan, Y., Guo, Z., Chen, W., Zhang, X., Han, Z., 2018. Deterministic-probabilistic approach for probable maximum typhoon-induced storm surge evaluation over Wenchang in the South China sea. Estuarine Coastal and Shelf Science 214, 161–172.
- Wu, R., Chen, X., Chen, D., Tu, Z., Zhang, G., Wang, D., 201. Investigation on current status of mangrove resources in Xinying Bay of Hainan Province. Chinese Journal of Tropical Agriculture 36, 35–37 (in Chinese with English abstract).
- Xin, K., Yan, K., Li, Z., Hu, J., Qiu, M., 2014. Distribution of soil organic carbon in mangrove wetlands of Hainan Island and its influencing factors. Acta Pedologica Sinica 51, 1078–1086 (in Chinese with English abstract).
- Xu, Y., Mead, R.N., Jaffé, R., 2006. A molecular marker-based assessment of sedimentary organic matter sources and distributions in Florida Bay. Hydrobiologia 569, 179–192.
- Xue, B., Yan, C.L., Lu, H.L., Bai, Y., 2009. Mangrove-derived organic carbon in sediment from Zhangjian Estuary (China) mangrove wetland. Journal of Coastal Research 25, 949–956.
- Yun, J., Deng, Y., Zhang, H., 2017. Anthropogenic protection alters the microbiome in intertidal mangrove wetlands in Hainan Island. Applied Microbiology and Biotechnology 101, 1–12.
- Zhang, Q., Chen, Y., 2003. Production and seasonal change pattern of litter fall of Rhizophora apiculata in Sanya River mangroves, Hainan Island. Acta Ecologica Sinica. 23 (in Chinese with English abstract).
- Zhang, Q., Sui, S., 2001. The mangrove wetland resources and their conservation in China. Journal of Natural Resources 16, 28–36 (in Chinese with English abstract).